

Dilatational Rheology of β -Casein Adsorbed Layers at Liquid–Fluid Interfaces

Julia Maldonado-Valderrama,^{*,†} Valentin B. Fainerman,[‡] M. José Gálvez-Ruiz,[†]
Antonio Martín-Rodríguez,[†] Miguel A. Cabrerizo-Vílchez,[†] and Reinhard Miller[§]

Grupo de Física de Fluidos y Biocoloides, Department of Applied Physics, University of Granada, Campus de Fuentenueva E-18071 Granada, Spain, Medical Physicochemical Center, Donetsk Medical University, 16 Ilych Avenue, 83003 Donetsk, Ukraine, and Max Planck Institut für Kolloid und Grenzflächenforschung, D-14424 Potsdam, Germany

Received: February 22, 2005; In Final Form: June 17, 2005

The rheological behavior of β -casein adsorption layers formed at the air–water and tetradecane–water interfaces is studied in detail by means of pendant drop tensiometry. First, its adsorption behavior is briefly summarized at both interfaces, experimentally and also theoretically. Subsequently, the experimental dilatational results obtained for a wide range of frequencies are presented for both interfaces. An interesting dependence with the oscillation frequency is observed via the comparative analysis of the interfacial elasticity (storage part) and the interfacial viscosity (loss part) for the two interfaces. The analysis of the interfacial elasticities provides information on the conformational transitions undergone by the protein upon adsorption at both interfaces. The air–water interface shows a complex behavior in which two maxima merge into one as the frequency increases, whereas only a single maximum is found at the tetradecane interface within the range of frequencies studied. This is interpreted in terms of a decisive interaction between the oil and the protein molecules. Furthermore, the analysis of the interfacial viscosities provides information on the relaxation processes occurring at both interfaces. Similarly, substantial differences arise between the gaseous and liquid interfaces and various possible relaxation mechanisms are discussed. Finally, the experimental elasticities obtained for frequencies higher than 0.1 Hz are further analyzed on the basis of a thermodynamic model. Accordingly, the nature of the conformational transition given by the maximum at these frequencies is discussed in terms of different theoretical considerations. The formation of a protein bilayer at the interface or the limited compressibility of the protein in the adsorbed state are regarded as possible explanations of the maximum.

1. Introduction

The rheological behavior of protein adsorption layers at liquid–fluid interfaces is an extremely complex phenomenon that has recently drawn the attention of many researchers.^{1–4} These dynamic properties are of fundamental interest in understanding the formation and stability of emulsions and foams.^{4,5} Upon adsorption to an interface, proteins partially unfold and rearrange within the interfacial layer.⁶ This feature substantially modifies the rheological properties of the layer as compared to those of usual surfactants.⁷ Furthermore, the structure of the adsorbed protein film not only depends on the stability of its native state^{8,9} but has been shown to be strongly influenced by the nature of the nonpolar phase onto which it is adsorbed.^{10–12}

The surface dilatational modulus is defined by the change in surface tension caused by a small deformation of the interface, and it is regarded as an important parameter during emulsification and foaming.⁵ Although Freer et al. point out the difficulty of interpreting the experimental dilatational results, they also state that the rheological parameters obtained from dilatational deformation of the interface are particularly revealing of the interfacial structure.⁸ As a matter of fact, with these parameters, the intrinsic softness or hardness of the protein as it unfolds and reconfigures at the interface can be inferred.⁶ In view of

all of these premises, the dilatational rheology technique was chosen in this study as the main experimental procedure.

Conjointly, the protein chosen in this research work was β -casein, a well-known model protein that is a key ingredient of dairy products.¹³ Certainly, due to its importance in the food industry, a great effort toward the understanding of the adsorption behavior of this protein can be found in the literature.^{2,8,13–19} However, among the dilatational studies performed with this protein at oil interfaces, to our knowledge, none of them cover a complete range of concentration and oscillation frequency which would very likely provide a rather complete picture of its adsorbed behavior.^{8,20}

Williams et al. were one of the first authors to report a comparative analysis of this protein's dilatational behavior at the air–water and paraffin oil–water interfaces by means of the ring-trough apparatus.¹⁵ Due to the experimental setup, the range of bulk concentrations considered varied only from 10^{-4} to 1 g/L and they show a plateau in the elasticity at the lowest concentration at both interfaces. As was already hypothesized by these authors, the elasticity should be zero when no protein is present. This assumption was subsequently probed by Benjamins et al. who effectively reported a maximum at the air–water interface and also at the tetradecane–water interface.⁷ In addition, Williams et al. hardly exposed differences between the behavior of β -casein at the air–water and paraffin oil–water interfaces.¹⁵ This similarity contrasts with Benjamins et al. findings in which a strong dependence of the protein's interfacial behavior on the nature of the nonpolar phase is

[†] University of Granada.

[‡] Donetsk Medical University.

[§] Max Planck Institut für Kolloid und Grenzflächenforschung.

observed.^{7,20} At any rate, since then, similar maxima have been reported at the air–water interface.^{14,16–18} However, the concrete mechanisms occurring at the interface have not yet been elucidated.

As a result, certain questions remain unsolved in the adsorption process of β -casein, especially at the oil interface. In particular, understanding the cited maxima in the elasticity modulus appears to be a major interest in this research work. Besides, since the interfacial viscosity of the layer contains information on the relaxation process, an explicit allusion to this magnitude and its dependence on frequency and interfacial coverage appears motivating. Therefore, a main objective of this research work was the accomplishment of a complete set of dilatational rheology experiments that would shed light on the referred phenomena. Furthermore, the elasticity and the viscosity of the interfacial layers formed at the air–water and oil–water interfaces are thoroughly analyzed independently with the purpose of highlighting the different information extracted from both parameters.

Concerning the above referred difficulty of extracting the structural information included in the dilatational experimental curves,⁸ a second objective of this study arises. In previous works, it was probed that the application of the thermodynamic model developed by Fainerman et al.^{21,22} to the experimental π – A adsorption curves provides further quantitative structural information on the interfacial layer.^{12,23} Recently, the authors have extended the formalism to the derivation of an expression of the Gibbs limiting elasticity on the basis of the same theoretical model.²⁴ Therefore, the application of the cited theoretical expression to the experimental results in order to clarify the experimental findings emerges as a second objective of this research work.

Accordingly, this work is structured as follows. First, previous results regarding the adsorption behavior of β -casein at the air–water and tetradecane–water interfaces are briefly reviewed. Subsequently, the experimental results of dilatational rheology of β -casein are presented for both interfaces and carefully analyzed. Finally, the static elasticity modulus obtained directly from the experimental curves is further analyzed on the basis of the referred thermodynamic model. Conclusively, a picture of β -casein's interfacial structure attained at both interfaces is proposed.

2. Theoretical Background

2.1. Equilibrium Adsorption. The theory of protein adsorption with changing partial molar area is described in detail in ref 21; however, a brief description will be given here. The theory is based on the idea of Joos and Serrien, in which proteins adsorb onto the interface with two different partial molar areas,²⁵ and generalizes it such that multiple states of the protein molecule can exist in the interfacial layer. Specifically, the model assumes that the partial molar area of the protein molecules can vary between a maximum, ω_{\max} , and a minimum, ω_{\min} , value that are determined by the geometrical dimensions of the protein. Besides, the molar areas of two “neighboring” conformations differ from each other by the value ω_0 . This incremental value is chosen to be equal to the molar area of the solvent, or the area occupied by one segment of the adsorbed protein molecule. Finally, the total number of possible states of the protein molecule, n , is fixed by the above-mentioned parameters so that $\omega_{\max} = \omega_1 + (n + 1)\omega_0$ and the molar area of the i th state is given by $\omega_i = \omega_1 + (i + 1)\omega_0$, where $1 \leq i \leq n$ and $\omega_{\min} = \omega_1$. It is assumed, also, that ω_0 is much smaller than the protein molar area in any state. In addition, these

limiting area values should take into account the ability of the protein molecule to unfold at the interface due to its molecular structure and also to the interaction with the nonpolar phase onto which it is adsorbed. This feature is addressed in detail in refs 12 and 23. With these premises and denoting the protein adsorption in the i th state as Γ_i , one obtains the total adsorption of proteins in all n states (i.e., the total adsorption of protein):

$$\Gamma = \sum_{i=0}^n \Gamma_i \quad (1)$$

so that the total surface coverage is expressed as

$$\theta = \omega \Gamma = \sum_{i=0}^n \Gamma_i \omega_i \quad (2)$$

The value ω represents the mean molar area defined as the weighted average over all states of protein in the interfacial layer.

The starting point of the thermodynamic analysis performed is Butler's equation for the chemical potentials of the i th state of a protein molecule within the interfacial layer and in the bulk solution.^{26,27} The equation of state based on a first-order model for both the nonideal entropy and the heat of mixing for the surface layer has been recently derived. Details on the derivation can be found in ref 21. The equation of state reads

$$-\frac{\pi \omega_0}{RT} = \ln(1 - \theta) + \theta \left(1 - \frac{\omega_0}{\omega} \right) + a\theta^2 \quad (3)$$

where R is the gas law constant, T is the temperature, and a is a Frumkin-type intermolecular interaction parameter.

The equations for the adsorption isotherm for each state (j) of the adsorbed protein are similarly obtained:

$$b_j c_0 = \frac{\omega \Gamma_j}{(1 - \theta)^{\omega_j/\omega}} \exp \left[-2a\theta \frac{\omega_j}{\omega} \right] \quad (4)$$

where c_0 is the concentration of the protein in the solution bulk and b_j is the adsorption equilibrium constant for the protein in the j th state. It can be assumed that the numerical values for all b_j are equal to each other within the limits $j = 1$ to $j = n$ so that the adsorption constant for the protein molecule as a whole is given by the sum $b = nb_j$.²¹ This feature allows each of the individual Γ_i to be expressed in terms of the total adsorption and, hence, provides the distribution function of adsorptions over various states of the protein molecule:

$$\Gamma_j = \Gamma \frac{(1 - \theta)^{(\omega_j - \omega_1)/\omega} \exp \left[2a\theta \frac{\omega_j - \omega_1}{\omega} \right]}{\sum_{i=1}^n (1 - \theta)^{(\omega_i - \omega_1)/\omega} \exp \left[2a\theta \frac{\omega_i - \omega_1}{\omega} \right]} \quad (5)$$

Finally, by introducing in this equation the average molar area of the protein ($\omega \Gamma = \sum_{i=1}^n \Gamma_i \omega_i$), one can derive

$$\omega = \frac{\sum_{i=1}^n \omega_i (1 - \theta)^{(\omega_i - \omega_1)/\omega} \exp \left[2a\theta \frac{\omega_i - \omega_1}{\omega} \right]}{\sum_{i=1}^n (1 - \theta)^{(\omega_i - \omega_1)/\omega} \exp \left[2a\theta \frac{\omega_i - \omega_1}{\omega} \right]} \quad (6)$$

This equation includes the relation between the interfacial coverage and the molar area of the protein. In particular, the states with smaller areas are favored at high interfacial coverages, whereas at extremely low interfacial coverages all of the adsorptions are equally probable.²¹

Accordingly, eqs 3–6 constitute a set of equations that describes very satisfactorily the adsorption behavior of proteins within the range of simultaneous increase of surface pressure and adsorption.^{21,28} For further concentrated solutions, the significant increase in adsorption without any noticeable change in the interfacial pressure^{29,30} can be explained either by taking into account a two-dimensional condensation within the protein layer³¹ or by assuming that a bilayer (or multilayer) is formed.^{32–35} For the latter case, the second layer would insignificantly affect the interfacial tension, and hence, the equation of state (eq 3) remains valid in the formalism. Subsequently, the isotherm equation for the bilayer adsorption is derived by assuming that the coverage of this layer is proportional to the adsorption equilibrium constant b_2 for the second layer and to the coverage of the interfacial layer. Hence, the second layer remains almost empty in the region of low interfacial coverage ($\Gamma < \Gamma^*$) as long as $b_2 < b_1$. The generalization of the adsorption isotherm for the region ($\Gamma < \Gamma^*$) reads³²

$$\Gamma\omega = \frac{b_1c_0}{1 + b_1c_0} \left[1 + \frac{b_2c_0}{1 + b_2c_0} \right] \quad (7)$$

Another possibility to describe the essential increase in adsorption for concentrated protein solutions consists of the possibility of an intrinsic compressibility of protein molecules in the state with minimal surface area, which can be expressed by the equation³⁶

$$\omega_1 = \omega_{10}(1 - \kappa\pi) \quad (8)$$

Here, the proportionality factor, κ , is the relative two-dimensional compressibility. It will be shown below that both models (bilayer and compressibility) predict almost identical characteristic dependencies of adsorption on concentration or interfacial pressure.

2.2. Gibbs Limiting Elasticity. The surface dilatational modulus is defined by the increase of surface tension for a small increase in the area of a surface element. This is in the general case a complex quantity with a storage part (elastic) and a loss part (viscous), resulting from a phase difference that occurs between dA and $d\pi$. In the limiting case, when there is no exchange of material with the adjoining bulk solution, that is, when $\Gamma \cdot A$ is constant, E_0 is called the Gibbs limiting elasticity. This situation can be achieved by performing oscillations at sufficiently high frequencies, so that no relaxation process can affect the surface tension within the time scale of the area oscillation. In this manner, the viscous component of the elasticity modulus can be neglected and the behavior of the interfacial layer is purely elastic.^{7,14,17}

$$E_0 = - \left(\frac{d\gamma}{d \ln \Gamma} \right) = \left(\frac{d\gamma}{d \ln A} \right) \quad (9)$$

at $\Gamma \cdot A = \text{constant}$.

Thus, in this limiting case, the elasticity can be deduced from the equilibrium equation of state. Differentiating eq 3 with respect to Γ , one obtains

$$E_0 = \left(\frac{d\pi}{d \ln \Gamma} \right) = \frac{RT}{\omega_0} \left[\frac{\theta}{1 - \theta} - \theta - 2a\theta \right] \left(1 + \frac{d \ln \omega}{d \ln \Gamma} \right) \quad (10)$$

where the dependence $d \ln \omega / d \ln \Gamma$ significantly affects the elasticity value.²⁴ Specifically, at high total surface coverage, the adsorption of molecules requiring a smaller area is favored at the expense of those requiring a larger area. This feature is reflected in the theoretical treatment by the exponential factor $(1 - \theta)^{(\omega_j - \omega_1)/\omega}$, in which $(\omega_j - \omega_1)/\omega > 0$. This implies that the probability of the existence of a protein molecule characterized by higher molar areas becomes essentially lower as the monolayer coverage increases. Accordingly, the dependence $d \ln \omega / d \ln \Gamma$ is < 0 . In this manner, eq 10 clearly fulfills a well-known experimental feature. Namely, the elasticity modulus of proteins, for which the cited relation holds, is essentially lower than that of molecules with constant molar area, for which the relation would be

$$E_0 = \left(\frac{d\pi}{d \ln \Gamma} \right) = \frac{RT}{\omega_0} \left[\frac{\theta}{1 - \theta} - \theta - 2a\theta \right] \quad (11)$$

Further detail on this treatment can be found elsewhere.²⁴

Finally, it will be shown in the discussion of the results how by inserting eq 7 into eq 10 the incidence of the bilayer formation can be tested on the experimental elasticity data as compared to the monomolecular layer described by eqs 3–6.

3. Experimental Section

3.1. Material. Lyophilized, essentially salt free bovine milk β -casein 90+ % by electrophoresis was purchased from Sigma Chemical Co. β -Casein is a model protein widely studied in the literature. It presents a random coil, asymmetric configuration and has an extremely flexible structure. It is made up of 209 amino acids, and it has a molecular weight of 23.8 kDa; the entire molecule has an average hydrophobicity of 5.58 KJ/res.³⁷ It was stored at -18°C and used without further purification. The oil phase used in this study is tetradecane (99+ %) purchased from Aldrich, purified with Florisil 60–100 mesh chromatography resins, and subsequently filtered with $0.2 \mu\text{m}$ poly(tetrafluoroethylene) (PTFE) filters. The aqueous subphase used is a 0.01 M phosphate buffer, prepared by mixing appropriate stock solutions of Na_2HPO_4 and NaH_2PO_4 with a final pH of 7. Also, 0.5 g/L of NaN_3 was added to the buffered solvent to prevent degradation processes. Solutions were prepared daily, and 0.054 μS Milli-Q+ purified water was used for buffer preparation and any other purposes. All experiments were performed at $T = 25^\circ\text{C}$. The surface tension, γ_0 , of the clean interface was measured before each experiment to ensure the absence of surface-active contaminants, obtaining values of 72.5–73 mN/m. Regarding the tetradecane, even after the purification method, it showed a low level of surface-active impurities. Still, they appeared at very long adsorption times, beyond the times of 10^4 s as used in the present studies. The purification process was repeated until the interfacial water–tetradecane tension remained between 51 and 53 mN/m.

3.2. Experimental Setup. All of the experiments were performed in a PAT1 drop profile tensiometer (Sinterface Technologies, Germany) and described in detail elsewhere.³⁸ In this device, the solution droplet is formed at the tip of a PTFE capillary which is immersed in a cuvette. The cuvette is filled either with a water saturated atmosphere (for the air–water interface experiments) or with the tetradecane, also saturated in water (for the oil–water interface experiments). The setup determines the characteristic parameters (volume, interfacial

area, and interfacial tension) by fitting experimental drop profiles, extracted from digital drop micrographs, to the Young-Laplace equation of capillarity by means of an algorithm described elsewhere.^{39,40} The computer controlled dosing system allows one to control a constant size of the drop during the experiment and also to induce area deformations. A sinusoidal perturbation is induced at the interface by injecting and extracting liquid into the drop. Subsequently, a Fourier transformation is performed on the data and the program provides as output the dilatational parameters of the interfacial layer, namely, the interfacial elasticity and viscosity.

The surface dilatational modulus upon compression and expansion is defined by the expression, first derived by Gibbs for the surface elasticity of a soap-stabilized film, as the change in surface tension produced by a small change in a surface area element. In the most general case, a perturbation of the interface results in a response of the interface of trying to re-establish the equilibrium. The response is represented by a complex quantity that accounts for a storage part and a loss part.⁴¹

$$E(i\omega) = E'(\omega) + iE''(\omega) = F\{\Delta\gamma(t)\}/F\{\Delta \ln A(t)\} \quad (12)$$

where $E' = \epsilon$ is the interfacial elasticity and $\eta = E''/\omega$ is the interfacial viscosity.^{5,28} Any spontaneous process occurring after the disturbance of the interface and directed toward the equilibration of the system can be described as a relaxation process. Since this involves the dissipation of energy, this is formally expressed in terms of the viscous component, η . Hence, when the viscosity is negligible, there are no energetic losses in the layer and the film behavior is purely elastic.⁵

The experiments were designed with the following protocol. First, the interfacial tension of a solution droplet was monitored at a constant interfacial area value for 10 h. After this period of time, changes in the interfacial pressure were scarcely detected anymore, and thus, the dilatational rheology experiments were performed under *equilibrium* conditions, by imposing area perturbations. Each perturbation consists of eight sine waves, at a fixed frequency followed by 10 min of constant interfacial area recording. In this way, eight perturbations at different frequencies were subsequently imposed. The frequencies chosen in this study are the following: 0.005, 0.01, 0.02, 0.04, 0.08, 0.1, 0.14, and 0.2 Hz. In this manner, the oscillations are slow enough so that the drop maintains its Laplacian shape and the algorithm used remains valid. Finally, the drop volume change, that is, the amplitude of the oscillation, remained under 10% of the volume of the drop in order to guarantee linear rheological behavior and also avoid the destruction of interfacial structures.⁴²

4. Results and Discussion

A first step in understanding the behavior of proteins at interfaces is the analysis of the adsorption at constant interfacial area. Examination of this process provides important information on the interfacial structure attained by the protein. The adsorption of β -casein has been previously analyzed in detail at the air–water and tetradecane–water interfaces on the basis of the theoretical model described in section 2.1. The reader interested in this study is referred to recent publications.^{12,23} Anyhow, due to the significant conclusions obtained in those works, the main results will be briefly summarized in order to facilitate a further understanding of the rheological behavior. Besides, the prior application of the thermodynamic model to the adsorption isotherm is required for the subsequent fitting of the elasticity data, as will be shown below.

Figure 1 shows the cited experimental adsorption isotherms as well as the theoretical fitting obtained from eqs 3–6 with

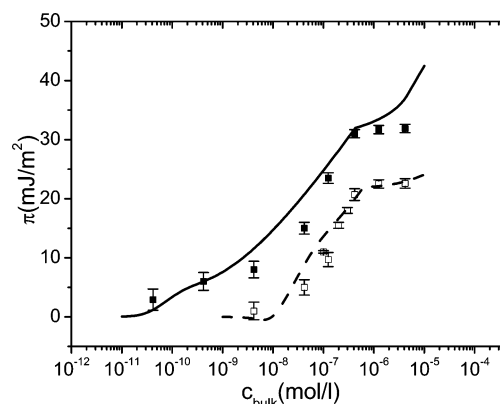


Figure 1. Experimental π – c isotherms for β -casein at the air–water (open symbols) and tetradecane–water (solid symbols) interfaces. Theoretical curves for the air–water (dashed line) and tetradecane–water (solid line) interfaces made with the parameters shown in Table 1 are also included.

TABLE 1: Equilibrium Fitting Parameters at the Air–Water and Tetradecane–Water Interfaces

	air–water	tetradecane–water
b_1	$3.5 \times 10^3 \text{ m}^3/\text{mol}$	$10^5 \text{ m}^3/\text{mol}$
b_2	$10 \text{ m}^3/\text{mol}$	$10^3 \text{ m}^3/\text{mol}$
a	1.00	0.50
ω_0	$2.5 \times 10^5 \text{ m}^2/\text{mol}$	$4.0 \times 10^5 \text{ m}^2/\text{mol}$
ω_{\min}	$4.5 \times 10^6 \text{ m}^2/\text{mol}$	$4.5 \times 10^6 \text{ m}^2/\text{mol}$
ω_{\max}	$4.5 \times 10^7 \text{ m}^2/\text{mol}$	$1.0 \times 10^8 \text{ m}^2/\text{mol}$

the parameters displayed in Table 1. The experimental data probe that the nature of the interface has substantially affected the properties of the interfacial layer formed at the tetradecane–water interface with respect to that formed at the air–water interface. The application of the theoretical model corroborates and, furthermore, quantifies these dissimilarities in terms of the different parameters used in the fitting procedure depending on the interface.^{12,23}

In particular, comparing the values given to the parameters at each interface, it can be seen how the value of the maximum partial molar area, ω_{\max} , increases at the tetradecane–water interface. Likewise, the value of the area occupied by one segment of the protein molecule at the interface, ω_0 , increases. Similarly, the value of b_1 increases at the oil interface, and this fact accounts for a higher affinity of the protein for the nonpolar phase.²¹ This feature is in agreement with the displacement of the isotherm at the tetradecane–water interface to lower bulk concentrations. Accordingly, the picture of the protein at the interface emerges as follows. On one hand, the hydrophobic chains of the adsorbed protein can penetrate into the oil phase, giving rise to a higher interfacial concentration, that is, a higher interfacial pressure at this interface for the same bulk concentration (Figure 1). This is due to the fact that the oil acts as a better solvent for the hydrophobic chains of the adsorbed protein than air or water, reducing the van der Waals interaction.^{2,10,42} On the other hand, the protein adopts a further unfolded state at the oil interface. To hinder the unfavorable interaction, resulting from the marked hydrophobic character of the oil, the protein tends to place itself at the interface and spread as much as possible so as to reduce the interfacial free energy (interfacial tension).^{11,12}

In Figure 2, the theoretical dependencies of adsorption, Γ , on interfacial pressure, π , are presented for β -casein at the tetradecane–water interface for all three models presented in section 2.1. Namely, the bilayer model, with all the parameters shown in Table 1, the monolayer model without condensation

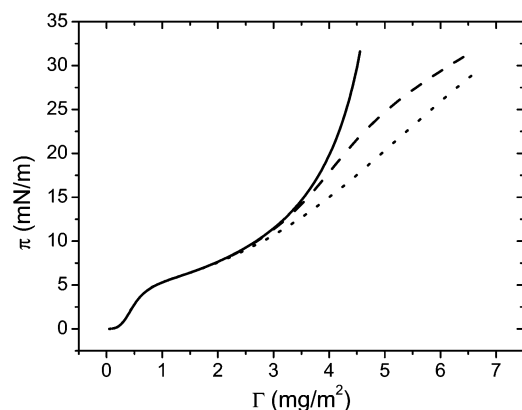


Figure 2. Theoretical dependencies of adsorption on interfacial pressure for β -casein at the tetradecane–water interface for three models: monolayer (solid line), bilayer (dashed line), and compressibility in the state of minimal area (dotted line).

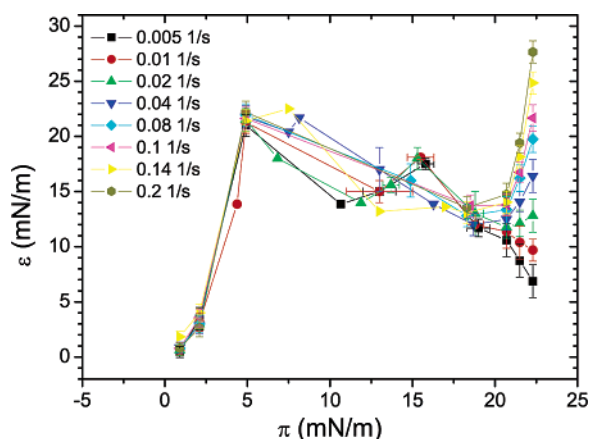


Figure 3. Interfacial elasticity of β -casein adsorbed at the air–water interface at various oscillating frequencies.

for $\pi > 32 \text{ mN/m}^{23}$ and $b_2 = 0$, and also the compressibility model which considers an additional compression in the state of minimal area ($b_2 = 0$, $\epsilon = 0.012 \text{ mN/m}$, and $\omega_{\min} = 6 \times 10^6 \text{ m}^2/\text{mol}$). It should be noted that the dependencies of interfacial pressure on concentration for all three models are also given in Figure 1. In this manner, it can be appreciated in Figure 2 that with increasing interfacial pressure the monolayer model yields a limiting adsorption of 4.5 mg/m^2 , whereas the two other models lead to an additional increase of adsorption with increasing interfacial pressure. The latter agrees better with the experimental data.^{29,30} Furthermore, the presence of inflection points in the dependence $\Gamma(\pi)$ results in extrema of the limiting (high frequency elasticity) E_0 . This important feature will be further analyzed below.

Once the adsorption behavior of β -casein has been characterized and bearing in mind the picture arising from such an analysis, one can interpret the dilatational experimental results. Figures 3 and 4 show the elasticity, ϵ , obtained for β -casein adsorption layers at the air–water interface and the tetradecane–water interface, respectively. Analogously, Figures 5 and 6 show, respectively, the viscosity, η , obtained for β -casein adsorption layers at the air–water and tetradecane–water interfaces.

At first glance, it can be seen how the elastic and viscous behavior of the layer are complementary in its frequency dependence at both interfaces. Namely, ϵ increases as the oscillating frequency increases, whereas η increases as the oscillating frequency decreases. Actually, at low frequencies, the protein has enough time to respond to the change in area.

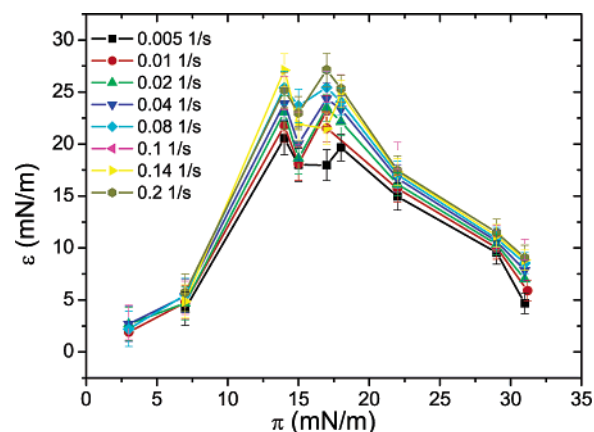


Figure 4. Interfacial elasticity of β -casein adsorbed at the tetradecane–water interface at various oscillating frequencies.

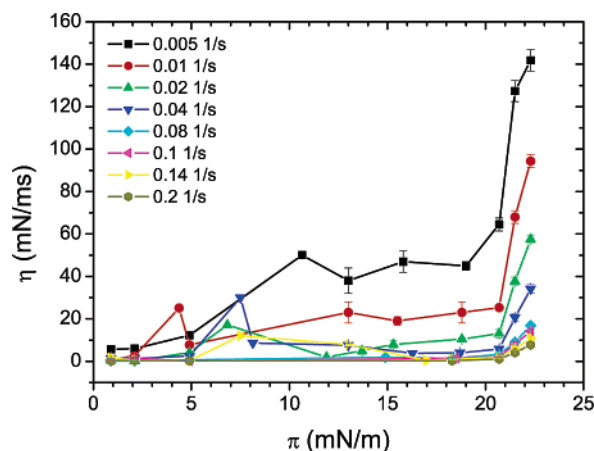


Figure 5. Interfacial viscosity of β -casein adsorbed at the air–water interface at various oscillating frequencies.

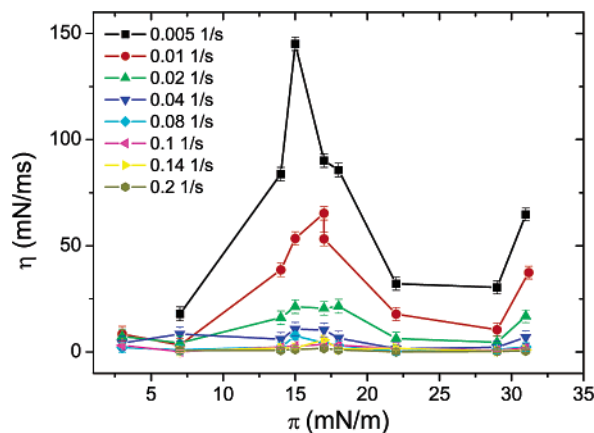


Figure 6. Interfacial viscosity of β -casein adsorbed at the tetradecane–water interface at various oscillating frequencies.

Hence, relaxation processes may occur within the layer and, simultaneously, the viscous behavior becomes noticeable. Conversely, as the frequency grows higher, the interfacial protein has less time to adapt to the deformation of the surface. Specifically, the elastic component of the layer increases, in detriment to the viscous behavior. Finally, at sufficiently high oscillating frequencies, the viscosity of the layer becomes negligible, and thus, above 0.1 Hz , the layer is considered to behave as purely elastic, as is stipulated in the literature.^{2,8,17,20,24}

However, the applied oscillation frequency seems to have a strong effect on the resulting dilatational behavior, as can be appreciated in the figures. Moreover, important differences

between both interfaces appear when comparing the respective dependence of the dilatational parameters with the interfacial coverage. It can be clearly seen also in Figures 3–6 how the dilatational behavior of β -casein is importantly affected by the nature of the nonpolar phase onto which it is adsorbed. To facilitate an understanding, let us analyze separately the elastic and viscous behavior of the interfacial layer.

First, we will look into the elastic behavior of the interfacial layer (Figures 3 and 4). Important differences arise between the two interfaces. A single maximum appears at the tetradecane–water interface whose height and width decrease with the oscillation frequency. Differently, two maxima are observed at the air–water interface that merge into one as the frequency of the oscillation increases. A maximum in the elasticity is linked with a conformational change within the interfacial layer.^{7,16,18} Therefore, it seems that the interfacial layer undergoes different structural transformations depending on the time given to the interface to adapt to perturbations of the interface, as given by the frequency. At the air–water interface, the appearance of two maxima in the elasticity has been previously reported for β -casein monolayers in refs 11, 16, and 18. In these studies, the layer was very slowly compressed so that the protein monolayer would have enough time to respond to the change in area. In agreement with those studies, in this case, the two maxima appear only at the lowest frequencies imposed. Cicuta et al. ascribe the first maximum to a collapse of trains into the subphase and the second to the formation of loops.¹⁸

As the frequency is further increased at the air–water interface, a single maximum results, located at approximately 7 mN/m. Similarly, the elasticity of the layer formed at the tetradecane–water interface shows one single maximum located at approximately at 15 mN/m. As a consequence, the location of this conformational change significantly depends on the type of interface. Accordingly, two different conformational regions can be distinguished in the adsorption process at the two interfaces studied, that appear separated by those maxima. Moreover, at the air–water interface, Miller et al. found a conformational transition located at a similar value of the interfacial pressure to the maximum shown in Figure 3.⁴⁴ In that work, the transition is interpreted as the formation of a second protein layer happening at that value of the interfacial coverage. Regarding the tetradecane–water interface, the displacement of the maximum to higher interfacial pressures indicates that a higher interfacial concentration is needed to undergo this conformational change. In our opinion, owing to the cohesive interaction between the hydrophobic chains and the oil, the protein would tend to place itself in contact with the oil rather than in subsequent adsorption layers, thus maybe delaying the formation of a second layer to higher interfacial pressures.

In addition, for interfacial pressures between zero and approximately 7 mN/m, the linear part of the elasticity is indicative of the compactness of the molecules at the interface.^{7,14,17,43} Concretely, the linear slope increases with decreasing flexibility of the protein. As can be seen in Figure 3, the slope is found to be higher at the air–water interface than the slope obtained at the oil–water interface, shown in Figure 4. On account of this, the structure adopted by β -casein at the oil interface is more flexible (soft) than the one at the air–water interface within this range of interfacial pressures and frequencies. Moreover, Hambardzumyan et al. report a similar lowering of the linear slope of the maximum with increasing temperature. Heating is known to denature the protein and, hence, promote its swelling in agreement with the decreasing slope.¹⁷ Similarly, the diminishing tendency of the elasticity shown for β -casein

at the tetradecane–water interface within the low pressure region might well be an indication of a further unfolding undertaken by the protein at this interface. This is completely in agreement with the theoretical analysis of the π – c isotherms shown above in which the further unfolded state attained by the protein at the oil interface is quantified by the application of the model.

Figures 3 and 4 show also that further increasing the interfacial pressure causes the value of the elasticity at the oil interface to exceed that at the gaseous interface. Moreover, due to the width of the maximum at the oil interface, even at low oscillating frequencies, the value overtakes that found at the air interface. Consequently, within this region, the film created at the tetradecane–water interface appears more resistant than that at the air–water interface.^{6,20} A possible explanation for the height of the maximum could be related to the presence of strong interactions between the hydrophobic segments of the protein and the oil phase, as has been elucidated by other authors.^{10,42} In addition, according to Hambardzumyan et al., van der Waals attractions play a major role in the elastic behavior of the layer. Consequently, the increase in elasticity found at the oil interface could be a result of an intensification of this type of interactions at this interface.

Second, let us examine the viscosity of the interfacial layers formed at the air–water and tetradecane–water interfaces shown in Figures 5 and 6. The onset of the viscous behavior marks the detection of relaxation processes occurring at the interface. Relaxation processes include the exchange of interfacial molecules with those located in subsurface layers, conformational molecular rearrangements occurring within the interface, or collapse phenomena.^{7,15,20,42}

By performing the analysis of the viscosity curves starting from the highest interfacial pressures, we can distinguish several regions. On one hand, at the highest interfacial pressures attained, both the air–water and tetradecane–water interfaces show similar increasing tendencies. The interfacial coverage is expected to be high within this interval, and hence, the relaxation process detected would correspond to exchange with molecules adsorbed in subsequent layers rather than to rearrangement within the interfacial layer. In this sense, Hambardzumyan et al. found a similar onset of the viscous behavior of the layer located at 17 mN/m for β -casein at the air–water interface which was not affected by an increase of temperature.¹⁷ Since the temperature substantially modifies the structure of the protein, this feature provides further evidence for the previous interpretation of the experimental data. Hence, the viscous behavior seems to occur regardless of the structure of the protein and might refer to whole molecules. Furthermore, the viscous component is found substantially higher at the air–water interface, indicating more energetic losses at this interface. The larger affinity of the protein for the tetradecane interface might well result in a higher cohesive interaction that prevents the exchange of molecules responsible for the viscous behavior of the layer. The partial solvation of the hydrophobic segments into the nonpolar phase also accounts for this feature. This is consistent with the elasticity values and the increasing resistance of the layer at the tetradecane interface found above. In this sense, Freer et al. found a similar increase of the viscosity of the interfacial layer formed by β -casein at the hexadecane–water interface.⁸ Similarly, they relate it to exchange of molecules within the multilayer structure attained at these interfacial pressures.

On the other hand, at lower interfacial coverages, the viscosity of the layer shows a maximum that appears to be more significant at the tetradecane–water interface. Moreover, a

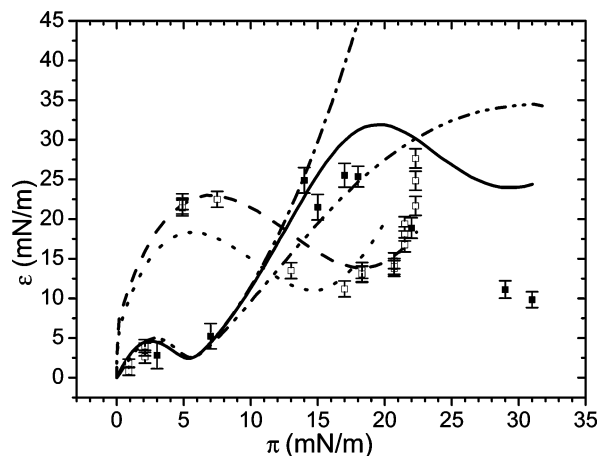


Figure 7. Experimental elasticity values for 0.1–0.2 Hz for β -casein at the air–water (open symbols) and tetradecane–water (solid symbols) interfaces. Theoretical curves made with the parameters shown in Table 1 for the air–water interface (dotted line, the monolayer model; dashed line, bilayer adsorption) and the tetradecane–water interface (dash-dotted line, the monolayer model; solid line, bilayer adsorption; dot-dot-dashed line, compressibility in the state with minimal area) are also shown.

remarkable viscosity is obtained only at the lowest oscillation frequencies imposed at both interfaces, in agreement with the theoretical predictions.⁵ Note that the amount of protein corresponding to the interfacial pressure where this maximum is located is very small. Therefore, it is unlikely that the relaxation processes detected at this point are related to the exchange of molecules as was the case before. Still, rearrangement of the protein within the interfacial layer might be more reasonable. Regarding the air–water interface, it seems to corroborate the collapse of segments of protein into the aqueous subphase given by the two maxima at these frequencies. Concerning the tetradecane interface, the important viscous component detected at the lowest oscillation frequencies might rather be related to interfacial unfolding. That is to say, the tendency of the protein to spread at the interface and the cohesive interaction between oil and protein results in an interfacial structure that is certainly “easier” to adapt to the interfacial perturbation sticking at the interface. In this manner, the interfacial unfolding process could be somehow favored at the oil interface with respect to that at the air–water interface in agreement with the larger area obtained from the theoretical model.

Finally, the experimental results shown in Figures 3–6 were analyzed on the basis of the theoretical considerations with the aim of further understanding the differences between the interfacial behavior of β -casein at the air–water and tetradecane–water interfaces. To apply eq 10 to the experimental data, one has to consider only those experiments in which the layer behaves as purely elastic, that is, when the viscosity is negligible. Thus, Figure 7 shows the experimental data obtained for the oscillation frequencies 0.1, 0.14, and 0.2 Hz for β -casein adsorption layers at the air–water and tetradecane–water interfaces. It can be appreciated in the figure that, within this range, the elasticity values are independent of the frequency imposed, accounting for the purely elastic behavior of the layer. In addition, Figure 7 shows the theoretical curves obtained by the application of the model (eq 10). Concretely, in this equation, two variations of the theoretical treatment have been included separately for the air–water interface and three variations for the tetradecane–water interface, namely, the monomolecular layer described by eqs 3–6, the formation of a second adsorption layer introduced in eq 7, and the additional compressibility of

protein molecules in the state with minimal surface area, with the latter being only for the oil interface. In this manner, the incidence of each mechanism on the adsorption process can be easily tested by comparison with the experimental data. It is worth noting that the parameters used in the calculations of the elasticity data are exactly the same as the parameters provided by the fitting of the respective adsorption isotherms and displayed in Table 1. Let us analyze in detail the conclusions arising from the analysis of the experimental elasticity data.

Regarding the curves obtained for the air–water interface, it was already shown in ref 24 that the inclusion of the bilayer approximation in the model barely modified the resulting curve with respect to the monomolecular film. However, the matching between theory and experiment is somehow improved with the consideration of the second layer, especially at the highest surface pressures. Besides, the values of E_0 for the air–water interface exhibit two extreme values corresponding to the kink in the experimental π versus Γ curve at $\Gamma \approx 1.2$ mg/m².²⁴ This phenomenon was first noted by Graham and Phillips who qualitatively ascribed it to a transition in the configuration from all trains to trains and loops.⁴⁵

At the tetradecane–water interface, let us analyze the incidence of each of the theoretical considerations on the experimental data in Figure 7. It can be seen how the consideration of a monomolecular interfacial film exhibits a deviation of the experimental data, whereas the correlation is importantly improved with the inclusion of additional mechanisms in the model. Similarly, Figure 2 shows how only the consideration of a bilayer or additional compressibility provides the predicted increase of adsorption with increasing concentration at the oil interface. Moreover, the appearance of an inflection point determines the position of a maximum in the limiting elasticity.²⁴ This feature is verified in Figure 7 in which the monomolecular film does not provide a second maximum in the elasticity at the oil–water interface, whereas the other two mechanisms each provide a maximum. Furthermore, the position of those maxima in Figure 7 completely match those of the respective inflection points. Note that the inflection point appears more remarkably by considering a bilayer formation and this feature is similarly reproduced in the shape of the maximum in the elasticity. On that account, the consideration of a bilayer in the theoretical treatment provides a substantially enhanced fitting of the experimental limiting elasticity. Therefore, it might be deduced from this analysis that a protein bilayer is formed at the tetradecane–water interface upon adsorption. Nevertheless, contrary to that at the air–water interface, at the tetradecane–water interface, the correlation between theory and experiments is merely qualitative and certainly diminishes with increasing interfacial coverage. The two-layer structure has been previously suggested in the literature for β -casein at the air–water and oil–water interfaces by means of ellipsometry,^{30,46} neutron reflection,⁴⁷ and octadecyltrichlorosilane (OTS) self-assembled monolayers.⁴⁸ However, other interfacial structures are also reported in the literature for the oil interface by means of dilatational rheology and interfacial tension techniques such as multilayer formation, interfacial aggregation, and interfacial gelation.^{8,9} At any rate, the lower viscosity found for the oil interface at the highest bulk concentrations added to the slight discrepancies encountered between theory and experiment at the oil interface might suggest that a mixed mechanism in which many phenomena such as bilayer/multilayer formation, interfacial aggregation, or interfacial gelation might take place.

The literature studies devoted to the interfacial structure adopted by β -casein at the air–water interface are much more

numerous than those at the oil–water interface. In this sense, it is certainly interesting to compare the conclusions arising from the comparison between theoretical and experimental results shown in Figure 7 with literature data of spread layers of β -casein. At the air–water interface, the values of E_0 calculated from the experimental dependence of surface pressure and area per molecule for β -casein practically coincide with the theoretical curve obtained for the air–water interface in Figure 7. That is to say, the maximum values of elasticity in both cases are approximately 20 mN/m and this maximum corresponds to a surface pressure of around 7 mN/m at the air–water interface. Both values are in agreement with several β -casein monolayer studies found in the literature.^{16,18,49,50} All of them ascribed this transition to the collapse of hydrophobic residues, expulsion of tails and loops, and formation of an entangled network. Similar conclusions arise from X-ray and neutron reflectivity measurements of β -casein adsorbed at the air–water interface.⁵¹

Besides, recent results of Brewster angle microscopy (BAM) and relative reflectivity have shown that at surface pressures higher than 10 mN/m the surface layer formed by β -casein does not only increase but also becomes inhomogeneous in its structure.^{49,50} Similarly, atomic force microscopy (AFM) studies reveal a greater layer thickness with increasing concentration accompanied by some overlapping of molecules that finally tend to form aggregates.⁵² This feature agrees with the conclusions drawn by the application of the model to the experimental data. In particular, the results presented in ref 24 show that at surface pressures above 10 mN/m a significant part of β -casein molecules in the surface layer are in a state of minimum area; see figure 2 in ref 24. It is probable that in such a state the protein molecules show a large tendency to aggregation or two-dimensional condensation, in contrast to molecules in a more unfolded state. The presence of such a variety of mechanisms can also be concluded from the analysis performed of theory and experiment in Figure 7 and suggests a similar occurrence at the oil–water interface that, however, still remains unsolved.

5. Conclusions

The presence of a nonpolar phase has an important effect on the rheological properties of β -casein adsorption layers. The comparative study performed at the air–water and tetradecane–water interfaces strongly accounts for this feature. The interfacial structure attained by the protein can be satisfactorily characterized in view of the results presented.

On one hand, the interfacial elasticity of the protein layer at the air–water interface is particularly dependent on the oscillating frequency. At high frequencies, the maxima encountered in the interfacial elasticity at both interfaces distinguish between two well-defined regions in the structural properties and mark the location of a configurational transition within the interfacial layer. At low interfacial coverage, the lower elasticity values obtained at the tetradecane–water interface suggest a further unfolded state attained by the protein due to the higher cohesive interaction between oil and molecules. As the interfacial coverage increases, this interaction results in a higher amount of protein adsorbed and a certain resistivity of the layer to collapse. The shift of the maxima to higher interfacial pressures at the tetradecane interface with respect to that at the air–water interface strongly supports this interpretation. At the lowest oscillating frequencies, the elasticity of the layer formed at the air–water interface shows two separated maxima. This finding agrees with literature data and is related to the collapse of protein segments into the subphase.

On the other hand, the two regions identified in the elasticity curves at high frequencies are characterized by a corresponding

viscous behavior. At high interfacial coverage, the relaxation detected at both interfaces is probably caused by the exchange of interfacial molecules between successive interfacial layers. At the tetradecane–water interface, the relaxation observed is lower due to the higher affinity of the protein to the nonpolar phase. At low interfacial coverage, the viscous behavior is noticeable at the lowest oscillating frequencies. At the air–water interface, the relaxation phenomena are clearly related to the collapse of segments into the subphase present in the elasticity curve. Furthermore, according to the elasticity data, the relaxation processes occurring in this region should be more likely to reorganize within the interfacial layer. The higher values obtained for the tetradecane–water interface suggest that the interaction between molecules and the nonpolar interface is higher and might well result in a further unfolded state attained by the protein upon contact with oil. Briefly, the dilatational deformation detects an intrinsically softer film formed at low interfacial coverage at the oil interface, whereas the resulting film as the interfacial coverage increases is found to be more resistant (elastic) than that at the air–water interface.

However, the concrete mechanisms happening at the interface remain somehow unclear with a too simplified interpretation of the experimental curves. Moreover, the observed features cannot be clarified by the application of the theoretical model to adsorption data only. Therefore, a consequent application of theoretical models to adsorption isotherms combined with elasticity data provides a remarkable improvement in the interpretation of the experimental findings. The former provides a quantification of the interfacial unfolding undertaken by the protein at each of the interfaces. The latter offers an accessible test of the incidence of an interfacial relaxation mechanism in the adsorption layer. Certainly, this procedure enables the extraction of important information hidden in the experimental elasticity and constitutes a promising tool in the understanding of the interfacial behavior of proteins. To be precise, the formation of a second protein layer arises as the predominant mechanism occurring upon collapse of the protein layer. Moreover, the noteworthy agreement found between theory and experiment by using the parameters provided by adsorption isotherm models probes the reliability of the theoretical treatment. As a consequence, the fitting procedure proposed shows a significant potential for the interpretation of experimental elasticity data of proteins at fluid interfaces.

Acknowledgment. Financial support from “Ministerio de Ciencia y Tecnología, plan nacional de investigación científica, desarrollo e innovación tecnológica (I+D+I)”. Projects AGL2001-3483-C02-02, MAT2004-06872-C03-01, and AGL2004-01531 are gratefully acknowledged. Very special thanks to Sabine Sigmund for her invaluable help in the laboratory.

References and Notes

- (1) Bos, M. A.; Vliet, T. V. *Adv. Colloid Interface Sci.* **2001**, *91*, 437.
- (2) Benjamins, J. Ph.D. Thesis, Wageningen University, 2000.
- (3) Wilde, A.; Husband, F.; Gunning, P.; Morris, V. *Adv. Colloid Interface Sci.* **2004**, *108*, 63.
- (4) Murray, B. S. In *Proteins at liquid interfaces*, 1st ed.; Möbius, D., Miller, R., Eds.; Elsevier: Amsterdam, The Netherlands, 1998.
- (5) Langevin, D. *Adv. Colloid Interface Sci.* **2000**, *88*, 209.
- (6) Pereira, L. G. C.; Théodoly, O.; Blach, H. W.; Radke, C. J. *Langmuir* **2003**, *19*, 2349.
- (7) Benjamins, J.; Lucassen-Reynders, E. H. In *Proteins at liquid interfaces*, 1st ed.; Möbius, D., Miller, R., Eds.; Elsevier: Amsterdam, The Netherlands, 1998.
- (8) Freer, M. E.; Yin, K. S.; Fuller, G. G.; Radke, C. J. *J. Phys. Chem. B* **2004**, *108*, 3835.
- (9) Beverung, C. J.; Radke, C. J.; Blanch, H. W. *Biophys. Chem.* **1999**, *81*, 59.

- (10) Murray, B. S.; Nelson, P. V. *Langmuir* **1996**, *12*, 5973.
- (11) Maldonado-Valderrama, J.; Gálvez-Ruiz, M. J.; Martín-Rodríguez, A.; Cabrerizo-Vílchez, M. A. *Colloids Surf.*, A, in press.
- (12) Maldonado-Valderrama, J.; Martín-Molina, A.; Gálvez-Ruiz, M. J.; Martín-Rodríguez, A.; Cabrerizo-Vílchez, M. A. *J. Phys. Chem. B* **2004**, *108*, 12940.
- (13) Dickinson, E. *Colloids Surf.*, A **2001**, *20*, 197.
- (14) Hambardzumyan, A.; Anguie-Béghin, V.; Daoud, M.; Douillard, R. *Langmuir* **2004**, *20*, 756.
- (15) Williams, A.; Prins, A. *Colloids Surf.*, A **1996**, *114*, 267.
- (16) Mellem, M.; Clark, F. A.; Husband, F. A.; Mackie, A. R. *Langmuir* **1998**, *14*, 1753.
- (17) Hambardzumyan, A.; Anguie-Béghin, V.; Panaiotov, I.; Douillard, R. *Langmuir* **2003**, *19*, 72.
- (18) Cicuta, P.; Hopkinson, I. J. *Chem. Phys* **2001**, *114*, 8569.
- (19) Bantchev, G. B.; Schwartz, D. *Langmuir* **2003**, *19*, 2673.
- (20) Benjamins, J.; Cagna, A.; Lucassen-Reynders, E. H. *Colloids Surf.*, A **1996**, *114*, 245.
- (21) Fainerman, V. B.; Lucassen-Reynders, E. H.; Miller, R. *Adv. Colloid Interface Sci.* **2003**, *106*, 237.
- (22) Miller, R.; Fainerman, V. B. In *Proteins at liquid interfaces*, 1st ed.; Möbius, D., Miller, R., Eds.; Elsevier: Amsterdam, The Netherlands, 1998.
- (23) Maldonado-Valderrama, J.; Fainerman, V. B.; Aksenenko, E.; Gálvez-Ruiz, M. J.; Cabrerizo-Vílchez, M. A.; Miller, R. *Colloids Surf.*, A **2005**, *261*, 85.
- (24) Lucassen-Reynders, E. H.; Fainerman, V. B.; Miller, R. *J. Phys. Chem. B* **2004**, *108*, 9173.
- (25) Joos, P.; Serrien, G. J. *J. Colloid Interface Sci.* **1991**, *145*, 291.
- (26) Fainerman, V. B.; Miller, R.; Wüstneck, R. *J. Colloid Interface Sci.* **1996**, *183*, 26.
- (27) Fainerman, V. B.; Lucassen-Reynders, E. H.; Miller, R. *Colloids Surf.*, A **1998**, *143*, 141.
- (28) Miller, R.; Fainerman, V. B.; Makievski, A. V.; Krägel, J.; Grigoriev, D. O.; Kazakov, V. N.; Synyachenko, O. V. *Adv. Colloid Interface Sci.* **2000**, *86*, 39.
- (29) Graham, D. E.; Phillips, M. C. *J. Colloid Interface Sci.* **1979**, *70*, 415.
- (30) Grigoriev, D.; Fainerman, V. B.; Makievski, A. V.; Krägel, J.; Wüstneck, R.; Miller, R. *J. Colloid Interface Sci.* **2002**, *253*, 257.
- (31) Fainerman, V. B.; Miller, R. *Langmuir* **1999**, *15*, 1812.
- (32) Miller, R.; Arsenenko, E. V.; Fainerman, V. B.; Pison, U. *Colloids Surf.*, A **2001**, *183*, 381.
- (33) Douillard, R.; Lefebvre, J. *J. Colloid Interface Sci.* **1990**, *139*, 488.
- (34) Douillard, R.; Daoud, M.; Lefebvre, J.; Minier, C.; Coutret, J. *J. Colloid Interface Sci.* **1994**, *163*, 277.
- (35) Guzman, R. Z.; Carbonell, R. G.; Kilpatrick, P. K. *J. Colloid Interface Sci.* **1986**, *114*, 536.
- (36) Fainerman, V. B.; Kovalchuk, V. I.; Aksenenko, E. V.; Michel, M.; Leser, M.; Miller, R. *J. Phys. Chem. B* **2004**, *108*, 13700.
- (37) Segumpta, T.; Razumovsky, L.; Damodaran, S. *Langmuir* **1999**, *15*, 6991.
- (38) Loglio, G.; Pandolfini, P.; Miller, R.; Makievski, A. V.; Ravera, F.; Ferrari, M.; Liggieri, L. In *Novel Methods to Study Interfacial Layers*, 1st ed.; Möbius, D., Miller, R., Eds.; Elsevier: Amsterdam, The Netherlands, 2001.
- (39) Maze, C.; Burnet, G. *Surf. Sci.* **1969**, *13*, 451.
- (40) Maze, C.; Burnet, G. *Surf. Sci.* **1971**, *24*, 335.
- (41) Lucassen, J.; Tempel, M. V. D. *J. Colloid Interface Sci.* **1972**, *41*, 491.
- (42) Wüstneck, R.; Moser, B.; Muschilok, G. *Colloids Surf.*, B **1999**, *15*, 263.
- (43) Anguie-Béghin, V.; Leclerc, E.; Daoud, M.; Douillard, R. *J. Colloid Interface Sci.* **1999**, *214*, 143.
- (44) Miller, R.; Fainerman, V. B.; Arsenenko, E. V.; Leser, M.; Michel, M. *Langmuir* **2004**, *20*, 771.
- (45) Graham, D. E.; Phillips, M. C. *J. Colloid Interface Sci.* **1980**, *76*, 227.
- (46) Russev, S. C.; Arguirov, T. V.; Gurkov, T. D. *Colloids Surf.*, B **2000**, *19*, 89.
- (47) Dickinson, E.; Horne, D. S.; Phips, J. S.; Richardson, R. M. *Langmuir* **1993**, *9*, 242.
- (48) Fragneto, G.; Thomas, R. K.; Rennie, A. R.; Penfold, J. *Science* **1995**, *267*, 657.
- (49) Rodríguez Patino, J. M.; Sanchez, C. C.; Rodríguez Nino, R. *Food Hydrocolloids* **1999**, *13*, 401.
- (50) Sanchez, C. C.; Rodríguez Nino, R.; Rodríguez Patino, J. M. *Colloids Surf.*, B **1999**, *12*, 161.
- (51) Harzallah, B.; Anguie-Béghin, V.; Douillard, R.; Bosio, L. *Int. J. Biol. Macromol.* **1990**, *23*, 73.
- (52) Bantchev, G. B.; Schwartz, D. K. *Langmuir* **2004**, *20*, 11692.